University Library



A gateway to Melbourne's research publications

Minerva Access is the Institutional Repository of The University of Melbourne

Author/s:
Perera, JS;Lam, N;Disfani, MM;Gad, E

Title:
Experimental and Analytical Investigation of a RC Wall with a Gabion Cushion Subjected to Boulder Impact

Date:
2021-05-31

Citation:
Perera, J. S., Lam, N., Disfani, M. M. & Gad, E. (2021). Experimental and Analytical Investigation of a RC Wall with a Gabion Cushion Subjected to Boulder Impact. INTERNATIONAL JOURNAL OF IMPACT ENGINEERING, 151, https://doi.org/10.1016/j.ijimpeng.2021.103823.

Persistent Link:
https://hdl.handle.net/11343/310876

Experimental and Analytical Investigation of a RC Wall with a Gabion Cushion Subjected to Boulder Impact

Jude Shalitha Perera[a]

[a] Department of Infrastructure Engineering, The University of Melbourne

Parkville, VIC, 3010, Australia. pjude@ unimelb.edu.au +61 0451570785 (Corresponding Author)

Nelson Lam[b]

[b] Department of Infrastructure Engineering, The University of Melbourne

Parkville, VIC, 3010, Australia. ntkl@ unimelb.edu.au

Mahdi Miri Disfani[c]

[c] Department of Infrastructure Engineering, The University of Melbourne

Parkville, VIC, 3010, Australia. mahdi.miri@unimelb.edu.au

Emad Gad[d]

[d] Faculty of Science, Engineering & Technology, Swinburne University of Science and Technology, Hawthorn, VIC, 3122, Australia. egad@swin.edu.au

Abstract

An experimental investigation involving the use of a full-scale pendulum device to deliver solid object impact on a reinforced concrete (RC) barrier specimen that was fitted with a layer of gabion cushion is reported in this paper. The deflection behaviour of the stem wall of the RC barrier including the tensile strains developed in the longitudinal reinforcement was of interests. Results recorded from the tests are compared with results from control experiments which were without the protection of any cushion materials. The introduction of a layer of cushion is shown to be able to have the contact force reduced by more than 95% and deflection demand reduced by about 70%. An analytical procedure employing the Hunt and Crossley contact model, Swiss code model and two-degrees-of-freedom (2DOF) system modelling technique is presented for calculating the flexural response behaviour of the cushioned barrier and validated by comparison with experimental measurements. An important outcome from the study is a simple hand calculation procedure featuring the use of a closed form expression along with a design chart which is illustrated by a worked example, to facilitate uptake in design practices.

Keywords: impact action, rockfall, impact barrier, gabion cushion

Acknowledgement

Financial support from the Australian Research Council (ARC) Discovery Project DP170101858 entitled “New Approach for Design of Barriers for Impact” is gratefully acknowledged. This paper is published with the permission of the Head of the Geotechnical Engineering Office and the Director of Civil Engineering and Development, Hong Kong SAR Government.

Notations

A_{st} = total area of reinforcement at tensile side
B = wall length
COR = coefficient of restitution

d = distance between compressive surface of concrete and centre of tensile bar
D = depth of concrete section
D_l = linear damping factor
D_n = nonlinear damping factor
e = thickness of cushion layer
E = Elastic modulus of concrete
EI_{cr} = flexural rigidity of cracked concrete
f_c' = compressive strength of concrete
f_y = tensile strength of reinforcement
F_c = contact force
F_{cmax} = maximum contact force
h = wall height
h_i = vertical distance between point of impact and axis of rotation
k = stiffness of the target responding within the elastic limit
k_{cr} = cracked stiffness
k_l = stiffness of frontal spring in linear visco-elastic 2DOF model
k_n = stiffness of frontal spring in non-linear visco-elastic 2DOF model
m = impactor's mass
m_2 = combined mass of the wall and cushion
m_{wall} = idealised lumped mass representing the reinforced concrete wall
m_{gabion} = contributory mass of the cushion
M_E = modulus of elasticity of the gabion layer
M_y = yield moment capacity of the reinforced concrete wall section
M_u = ultimate moment capacity of the reinforced concrete wall section
p = exponent characterising the non-linearity of spring
r = radius of equivalent sphere
r_1 = radius of the force transmitted area
T_m = time taken for the contact force to rise to its peak
T_{m2} = time taken by the target to deflect to the full extent
v_0 = impact velocity
v_1 = velocity of the impactor after the impact
v_2 = velocity of the target after the impact
δ = indentation of impactor into surface of target (linear)
δ_{max} = maximum indentation
$\dot{\delta}$ = velocity of indentation
$\dot{\delta}_0$ = relative velocity between two colliding objects at initial contact
Δ = maximum deflection of cantilevered wall
Δ_y = deflection of stem wall at yield limit
Δ_{yi} = deflection of stem wall at the point of impact at yield limit
γ = reduction factor
ρ = density of the gabion cushion
ε_s = maximum tensile strain of reinforcement
ε_{sy} = yield strain of reinforcement

ϕ = bending curvature of the reinforced concrete wall
ϕ_y = yield curvature of the reinforced concrete wall
ϕ_k = internal friction angle of particles
λ = ratio of the target mass to the impactor mass
λ_2 = ratio of the combined target mass to the impactor mass

1 Introduction

Dwellings built in mountainous areas can be vulnerable to rockfall and landslide hazards. In areas that are subject to such hazards including many parts of Switzerland, France, Italy, Japan and some overly congested metropolitan areas across Asia (e.g. Hong Kong) protective structures such as earth dams, rockfall sheds and reinforced concrete (RC) barriers have been erected to provide protection. Earth dams are massive, intrusive and require ample accessible space to build thereby posting safety issues in mountainous areas. RC barriers and rockfall sheds occupy much less space than earth dams but require a layer of materials to be placed on surfaces that are exposed to impact by boulders to function as "cushion". For example, rockfall sheds (that are commonly found in mountainous roadways in Switzerland) are typically covered by a layer of gravel to cushion the impact of falling rocks [1].

Gabions are rectangular steel cages made of hexagonal double twisted wire mesh or square welded wire mesh filled with appropriately sized rock particles and then stacked in front of a RC barrier to provide additional protection. The effectiveness of the gabion cushion layer in enhancing the impact-resistant capacity of a barrier has been investigated in Refs. [2-4]. This cushion layer is normally designed to reduce the intensity of the contact pressure that is potentially generated by the impact of a falling boulder in view of the risks of the RC protective slab/barrier being punched through at the point of contact [5-8]. In addition to controlling the contact pressure, the cushion layer also mitigates impulsive action transmitted to the barrier [9].

There are number of experimental studies available in the literature on the effectiveness of the gabion cushion layer. Some of these experimental arrangements used a soil embankment as the structural component [2, 3] and some used a concrete wall as the structural element [4]. In an

investigation reported in Ref. [10] several layers of gabions made up of different materials (forming a sandwich structure) were offered as a promising technical solution for countering rockfall hazards. However, Improvements to the flexural performance behaviour of the structure resulted from the transmitted impulsive action have never been considered. Recognising this knowledge gap, the authors performed a full-scale test on RC barrier specimen. The cantilevered RC wall was impact tested by a pendulum device. Full-scale unconfined compression testings of the gabion were also performed alongside impact experiments to characterise the properties of the gabion. Influence by the type of infill and cage strengths have also been studied. In addition to studying the contact force behaviour, the experimental investigation was also aimed at quantifying the influence of the gabion cushion on the deflection demand of the stem wall resulted from the impulsive action. Barriers that are with, and without, protection by gabions were tested to compare their respective contact force, deflection demand and reinforcement strains generated by the impact.

Alongside the impact experiments, an analytical procedure for guiding the structural design of RC rockfall barriers that are protected by gabions has also been derived. The development of the analytical methodology involved a two-degree-of-freedom (2DOF) spring connected lumped mass model featuring the use of the Hunt and Crossley model (to define the hysteretic properties of the frontal spring representing the cushioning action of the gabions). The forcing function of the impact and the resulting deflection of the stem wall can be predicted using the analytical model which was then validated by experimental measurements from full scale testings. A hand calculation procedure based on displacement principles is introduced at the end of the article, illustrated with a worked example. The procedure involves the use of a design chart to facilitate determination of the cushion reduction factor.

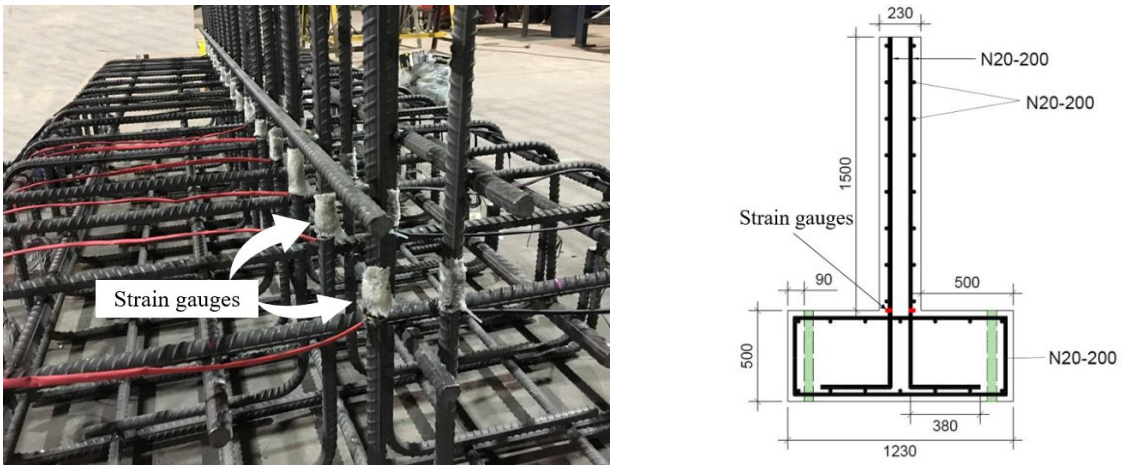
2 Full Scale Horizontal Impact Tests

In practice RC barriers vary in size considerably depending on site conditions and the nature of the rockfall hazard. The decision made on the dimensions of the barrier specimen that was tested by the authors was to ensure that the manner of casting the wall and the type of materials used were consistent with that of a real RC barrier. The stem wall of the test barrier was 230 mm thick and 1.5 m tall and was reinforced with 20 mm diameter reinforcing bars with 40 mm cover. These dimensions were sufficiently large to fulfill the stated criterion. The length of the barrier was selected as twice the height of the wall (which is 3 m) and the rationale behind the selection of this length is explained under Section 4.3. A second model barrier is presented in Appendix A as worked example to illustrate the proposed calculation methodology is of a much larger dimension. In view of the frequent occurrences of impact by boulders the test specimen was designed not to surpass the yield limit.

The RC wall was cast on a base slab of 0.5 m thick and 1.23 m long. Grade D500N, 15 tensile and 15 compressive reinforcing steel bars were used as vertical and horizontal reinforcement in the cantilevered wall (Fig. 1). Similar reinforcement arrangement was used for the base slab to ensure that the cantilevered wall was fixed rigidly to the foundation which was in turn held firmly onto the strong floor of the laboratory. Strain gauges for high elongation strain measurements in post yield conditions were attached to the base of the wall (refer Fig. 1 for the exact location) on each vertical steel bars prior to the casting of the concrete; 30 strain gauges were deployed in total to instrument the test wall (15 on each side). Data recorded from the strain gauges were acquired at a rate of 2 kHz during cyclic stress reversals.

The test wall was cast of concrete with maximum aggregate size of 20 mm, characteristic (28 days) compressive strength exceeding 40 MPa and density of 2400 kg/m^3 approximately. Compression tests were carried out on six concrete cylinders during the time the impact tests were carried out. Cylinders were tested in different time intervals (after 28 days, 2 days before

the beginning of the test and two weeks after the test). The concrete strength was found to not vary significantly across the six tests, and the test results averaged at 47 MPa.



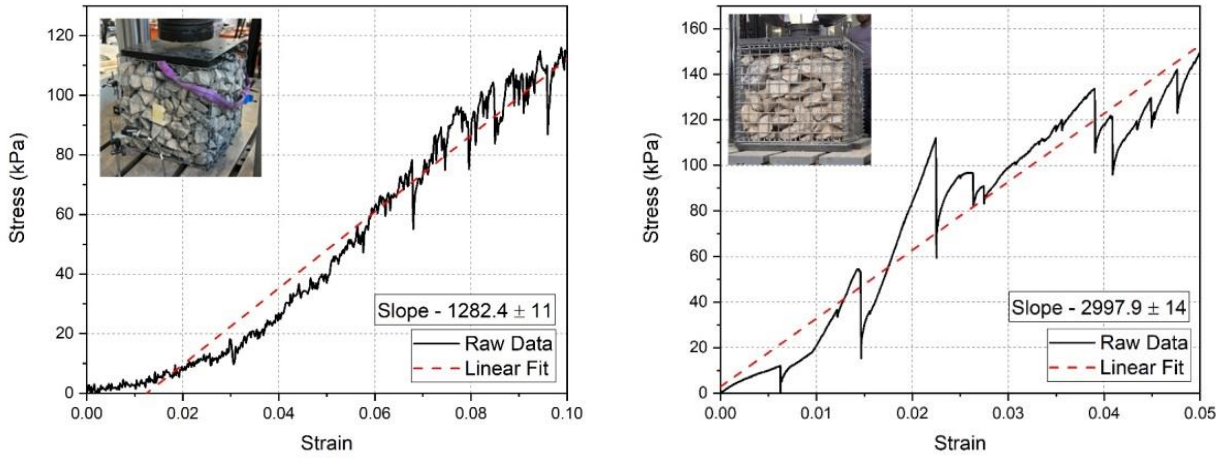
(a) Reinforcement with strain gauges attached (b) Detailed drawing

Fig. 1 Details of the reinforced concrete wall

Typical size of a gabion box could vary from 500 mm to 1000 mm along the width and 500 mm to 2000 mm along the length directions. The gabions selected for this experiment were cubical in shape and with side dimensions of 500 mm. Any stone or other material may be used to fill the gabion but to ensure the durability of the structure the infill material must be durable, sufficiently hard, weather-resistant, non-friable and insoluble. The most used materials are river stones or quarried stones. The most appropriate size for infill stone varies from 1 and 1.5 to 2 times the dimension of the opening of the mesh to prevent losses of material [11]. Two types of infill materials: crushed gravel (70 - 100 mm) and river pebbles (50 - 200 mm) were used in this test. The relatively flexible gabion cages had wire mesh of 3 mm in diameter (with 75 mm square openings) whereas stronger cages had wire mesh of 5 mm in diameter (with 50 mm square openings).

The average gabion box weighted 210 kg and 215 kg for crushed gravel and river pebbles fills, respectively. The bulk density of a gabion box was accordingly 1451 kg/m^3 for a gravel filled gabion and 1486 kg/m^3 for river pebbles filled gabion. Static tests in unconfined conditions were carried out on specimens of the gabion boxes to obtain their stiffness properties. The test results

are expressed in terms of the modulus of elasticity. Each gabion box was loaded quasi-statically by an actuator which was rated at 1 MN (MTS 311.31) as shown in Fig. 2. A 32 mm thick steel plate was placed on top of the gabion box to distribute the compressive force evenly on its upper surface. Compression strains of up to 0.2 were applied at a rate of 1 mm/s. Two tests were conducted for each type of fill materials for the flexible gabions, and four tests for each type of fill materials for the stronger gabions. Modulus of elasticity (M_E) of the gabions was inferred from test results based on the average slope of the stress-strain diagram as illustrated in Fig. 2. The compressive stiffness of the gabion box was mainly dependant on the strength of the box. With flexible gabions an average M_E value of 1172 kPa was recorded. With the stronger gabions a higher M_E value of 2985 kPa was recorded. For calculation purposes the value of M_E was rounded up to 1200 kPa for the flexible gabions and 3000 kPa for the stronger gabions.

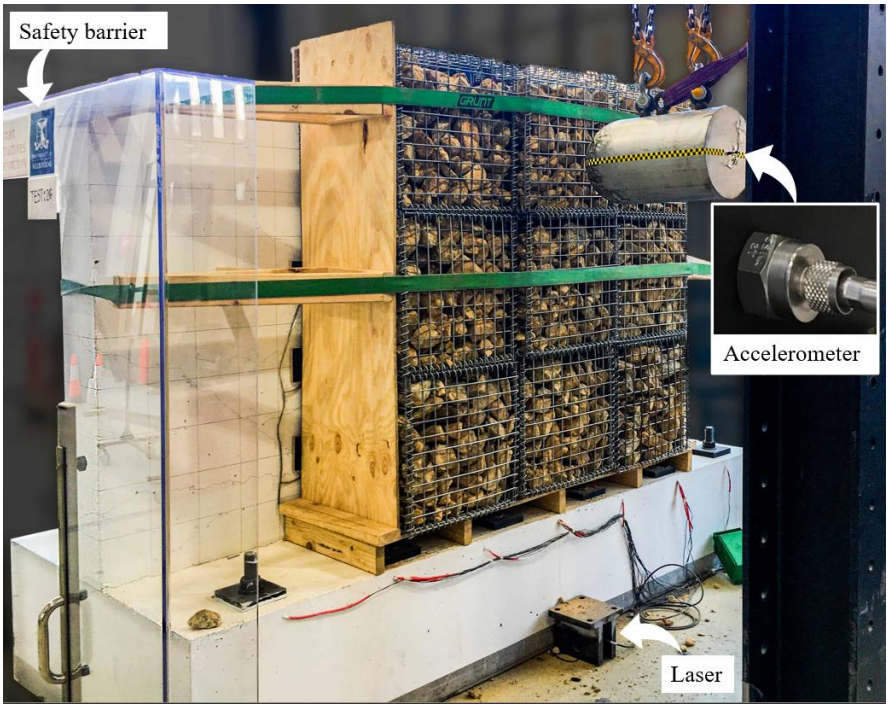


(a) Flexible gabion (b) Strong gabion

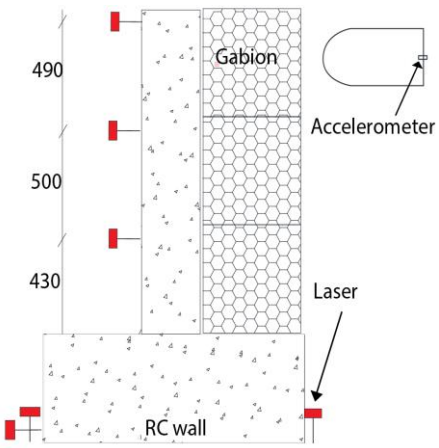
Fig. 2 Unconfined compression test

In the full-scale impact test setup, nine gabions were placed in a 3 by 3 matrix which was surrounded by a frame made of 17 mm thick plywood for holding the gabions in position. A plywood stage was used at the base to prevent any contact of the gabions with the threaded rods that were used to hold the base slab down onto the strong floor of the laboratory. The frame and gabions were then secured to the cantilevered wall using truck lashing belts. A photograph displaying an overview of the test set-up including the RC wall specimen, gabion cushion layer, the impactor object and details of the instrumentation is shown in Fig. 3.

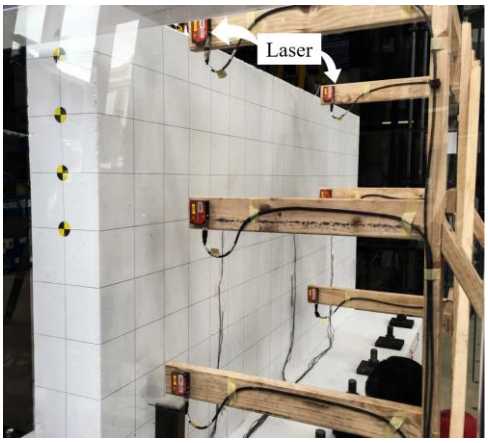
Three “torpedo” shaped impactors weighing 280 kg, 435kg and 1020 kg (for impactor “1“, “2” and “3” respectively) were made of solid steel and had their “contact end” (the end for striking the target) machined into a hemispherical surface (with diameters 150 mm, 150 mm and 200 mm respectively). An accelerometer (Model: 3200B6M by Dytran) with measurement capacity of up to 2500 g was screwed onto the flat end of the steel impactor to record its acceleration time-history (Fig 3 (a)). The amount of contact force generated by the impact could then be calculated. The accelerometer had frequency response of up to 10 kHz. A high-speed camera (model Phantom v2512) was used to capture images taken at the location of contact, and to record the velocity of the impactor at all stages of the impact from initial contact through to re-bounce. Model ILD 1302 laser sensors (Micro-Epsilon) with measurement frequency of up to 750 Hz were employed for capturing the motion of the test wall. Laser sensors were attached to a timber frame to take measurements at the following locations on the rear face of the test wall at the centreline and at the edge: (i) close to the upper edge, (ii) at two-thirds height, (iii) at one-third height and (iv) close to the ground surface (Fig. 3 (c)). Additional laser sensors were used to detect movement, if any, of the base slab (Fig. 3 (b)).



(a) Front side of the test set up



(b) Details of the instruments



(c) Side view of the set up

Fig. 3 Overview of the test set up

Four impact experiments were carried out initially as control experiments featuring the use of a protective steel plate (dimensions: 500 mm x 500 mm x 32 mm) which was attached to the stem wall at the location where the impactor was to strike (i.e. 150 mm below the upper end of the wall at the centreline). The protective plate was installed to ensure that the bending behaviour of the wall was comparable across multiple tests without being distorted by cumulative localised damage surrounding the point of contact. A total of nine impact experiments were conducted on the test wall which was protected by the gabion cushion. The point of impact was remained at the same height. The specimen experienced well distributed crack formation in order that its behaviour was consistently in a fully cracked state across all the tests. Crack distribution was monitored following every strike to ensure that no new cracks were formed when subject to subsequent strikes.

Solid steel impactors were lifted, and released, in separate tests to strike the gabion protected wall specimen. Details of the test setup in relation to the gabion cage, fill materials, impactor mass, drop height and impact energy are listed in Table 1. Test results including contact force, maximum deflection (measured by the laser pointing at the centerline closer to the upper edge of the wall) and maximum strain (measured at the middle of the wall) is also shown on the same table. Note that [**Test C1, 1, 3 and 5**], [Test C2, 2, 4 and 6], [*Test C3 and 7*] and [Test C4 and 8] were comparable in terms of the amount of energy delivered by the strike. Test 9 which had a

much higher energy demand (10 kJ) was performed to highlight the importance of installing a layer of gabions to protect a RC barrier in a real rockfall scenario.

Table 1 details of the full-scale test sequence

Test No.	Details of the gabion cage	Impactor mass (kg)	Height of Release (m)	Impact Energy (J)	Contact Force (kN)	Maximum Deflection (mm)	Maximum Strain
C1	No cushion – control experiment	280	1.4	**3846**	**1490**	**11.7**	**0.00190**
C2	No cushion – control experiment	435	0.58	2471	1110	12.3	0.00210
C3	No cushion – control experiment	280	0.5	*1374*	*920*	*4.9*	*0.00100*
C4	No cushion – control experiment	435	0.32	1374	800	9.2	0.00160
1	Flexible cage – crushed gravel	280	1.4	**3846**	**19.2**	**1.9**	**0.00024**
2	Flexible cage – crushed gravel	435	0.58	2471	15.8	1.3	0.00018
3	Flexible cage – pebbles	280	1.4	**3846**	**NA**	**2.5**	**0.00035**
4	Flexible cage – pebbles	435	0.58	2471	15.2	1.4	0.00019
5	Strong cage – crushed gravel	280	1.4	**3846**	**32**	**4.0**	**0.00068**
6	Strong cage – crushed gravel	435	0.58	2471	27	3.0	0.00050
7	Strong cage – crushed gravel	280	0.5	*1374*	*15*	*1.7*	*0.00027*
8	Strong cage – crushed gravel	435	0.32	1374	12.5	1.7	0.00021
9	Strong cage – crushed gravel	1020	1	**10006**	**64**	**5.5**	**0.00100**

One important finding of this full-scale test is that the peak contact force has been reduced significantly by the extra gabion cushion protection. It was found form deflection measurements of the wall that the use of gabion cushion has achieved some 50% to 90% reduction of the deflection of the wall. Same observations were reflected in the strain measurements as well which is of interest to the design engineer. It was also noticed that the stiffness properties of the gabion cushion (quantified through the unconfined compression test) has influenced not only the contact force, but also the deflection demand and tensile strain demand on the RC stemwall.

3 Modelling of the Contact Force

3.1 Existing Empirical Models for predicting contact force

A simple calculation procedure for predicting contact force generated by the impact of a fallen rock was proposed by Ng, Choi, Su, Kwan and Lam [4]. Their analysis was based on the Hertz elastic theory as summarized herein. The impact between a sphere of radius 'r' and a plane surface can be calculated based on the Hertz contact theory assuming elastic behaviour as shown by Eq. (1) [12]. The main drawback with the presented formulation was the misuse of Hertz law in Ref [14] as Hertz law should only be applicable where materials of the colliding objects are in the elastic state.

$$F_{cmax} = \frac{4E}{3} r^{\frac{1}{2}} (\delta_{max})^{\frac{3}{2}} \tag{1}$$

where E is the effective modulus of elasticity (in Pa) and can be taken as the modulus of elasticity of the cushion (M_E) when the stiffness of the cushion layer is significantly lower than that of the impactor. Maximum elastic indentation (δ_{max}) can be estimated using Eq. (2).

$$\delta_{max} = \left(\frac{15 m v_0^2}{16 E r^{\frac{1}{2}}} \right)^{\frac{2}{5}} \tag{2}$$

Substitution of Eq. (2) into Eq. (1) results in Eq. (3).

$$F_{cmax} = 1.25 M_E^{\frac{2}{5}} r^{\frac{1}{5}} m^{\frac{3}{5}} v_0^{\frac{6}{5}} \tag{3}$$

The main drawback of the presented formulation is that the effect of thickness of the cushion on the contact force has not been taken into account in the derivation of the expressions. There are contact force models available in the literature which consider the effect of thickness of the cushion layer and a comparison of the applicability of those models with the gabion cushion is studied by the author as given in Ref [13]. The empirical formula of Eq. (4) for estimating maximum contact force (F_{cmax}) as stipulated by the Swiss code [14] was found to be most

208 accurate and has a form similar to Eq. (3) with two additional terms namely the thickness of the
209 cushion layer (e) and the friction angle of the gabion fill ($tan\phi_k$).

$$F_{cmax} \sim 2.8 \times e^{-0.5} \times r^{0.7} \times M_E^{0.4} \times tan\phi_k \times \left(\frac{mv_0^2}{2}\right)^{0.6} \quad (4)$$

210 Guidelines stipulated in Swiss code [14] were derived from experimental studies performed by
211 Stoffel [15] and numerical analyses undertaken by Bucher [16]. A square-shaped slab of
212 dimensions: 3.4 m × 3.4 m × 0.2 m was subject to the impact of a dropped hemispherical
213 shaped steel shell filled with concrete. Three different layers of cushion materials comprised of
214 crushed concrete gravels, alluvial cones and scrap rocks were used to cover the concrete slab. It
215 was revealed from experimental and numerical investigations performed on hemispherical and
216 pyramidal shaped impactor objects that a hemispherical impactor induced higher impact force
217 and less penetration into the surface of the target [17]. Thus, the impact of a piece of rock (with
218 sharp corners) is expected to have lower deflection demand on the wall than what was recorded
219 from tests when other parameters were kept unchanged. Design methods developed using a
220 hemispherical shaped impactor object for cushioned impact is therefore conservative.

221 The modulus of subgrade reaction (M_E) in Eq. (3) and Eq. (4) is the key stiffness parameter for
222 input into the formulae. In the Swiss code both M_E and the internal friction angle $\tan\phi_k$ are
223 used as input parameters to characterise the mechanical properties of the cushion material. Plate
224 bearing test is recommended by Swiss Code [14] and Stoffel [15] for obtaining the value of M_E
225 experimentally. A M_E value of 3200 kPa is recommended for a layer of gravel by Labiouse,
226 Descoeudres and Montani [18], and this was essentially the same experiment used for
227 developing the Swiss code guidelines. No recommendation has been reported in the literature
228 for predicting the value of M_E for a gabion cage that contains gravel in a confined condition.
229 The level of compaction that could be achieved in the gabion could influence the value of M_E
230 and much depends on the infill particle properties, steel wire mesh properties and filling
231 methods. To obtain a more reliable estimate for the value of M_E it is recommended to conduct

static tests on a single box of gabion as explained in the previous section (in the form of an unconfined compression test) in order that specific properties of the gabion can be taken into account. The higher the assumed value of M_E the higher the predicted contact force value. A large number of static tests on full scale gabion specimens performed by Agostini [11] has contributed to the development of a design chart for obtaining the stress-strain relationship of a gabion. According to the test results, the value of M_E (modulus of elasticity) varied from 1000 kPa to 4000 kPa for unconfined conditions and about double the value for confined conditions [11, 19]. In the absence of static test results to characterise the properties of the gabion, a design chart as presented in Agostini [11] can be used to approximate the value of M_E of the gabion.

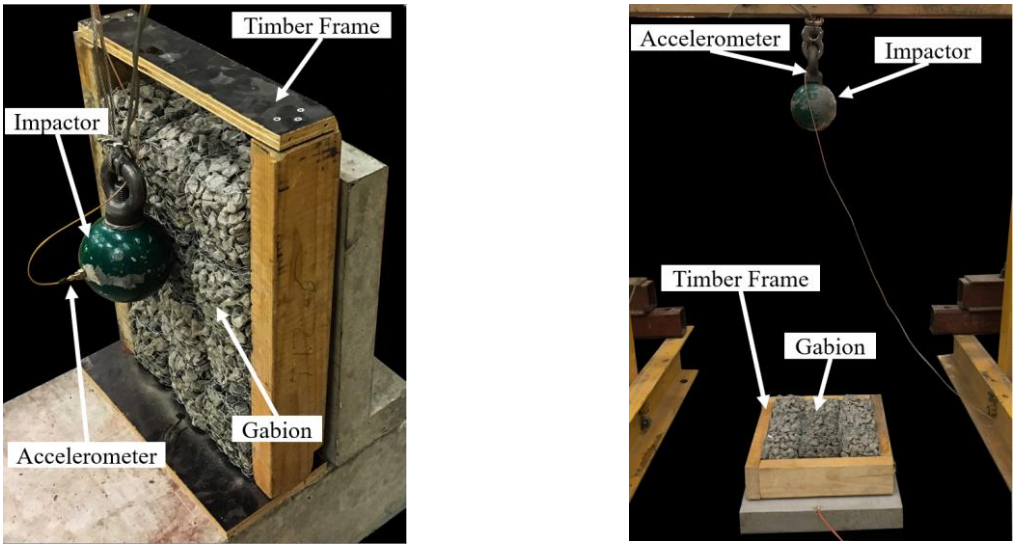
The coefficient is empirical in nature and was derived from results obtained from a vast number of drop tests where the layer of gravely particles were well confined [15]. In contrast to the experimental conditions used by Labiouse, Descoeudres and Montani [18] in deriving Swiss code equation, gabions filled with rock particles cannot be confined when stacked vertically and usually become loose when put in place. The validity of the Swiss code equations (Eq. (4)) in dealing with horizontal impact (as opposed to vertical impact with "drop testing" as was originally intended) and the influence of the gabion cage were uncertainties to be resolved given the change in confinement as the orientation of the test setup is changed. Therefore, the empirical formular of Eq. (4) would need to be re-evaluated for transverse impact on a vertical stack of gabions.

3.2 Modification factor to allow for change in orientation

Small-scale horizontal and vertical impact tests have been carried out using an array of gabions as shown in Fig. 4 to study the effect of confinement based on the orientation of the setup and the direction of impact. A 2500 g accelerometer (DJB A/123 Ts) which was fixed to the 5kg steel ball impactor was used for measuring the level of shock (de-acceleration) as contact was made with the gabions. The magnitude of contact force generated by the impact was obtained as

product of the de-acceleration and mass of the impactor. Gabion boxes were scaled down by 1:5 to be matched with the radius of the impactor. Both the steel wires and filling materials were scaled by the same factor. A timber frame was used to keep the gabions in place. The recorded contact force values were then compared and a contact force conversion factor of 0.65 was found as the impact was changed from vertical to horizontal orientation. The coefficient value of "0.65" was obtained through calibration against results from the horizontal strike tests on the gabion cushion. The conversion (reduction) factor so inferred from the comparison of the test results was used to modify the empirical formular (of Eq. (4)) to allow for change in orientation of the gabions in a horizontal impact scenario. The modified Eq. (5) is referred herein as the "Modified Swiss Equation".

$$F_{cmax} = 0.65 \times 2.8 \times e^{-0.5} \times r^{0.7} \times M_E^{0.4} \times tan\phi_k \times \left(\frac{mv_0^2}{2}\right)^{0.6} \quad (5)$$

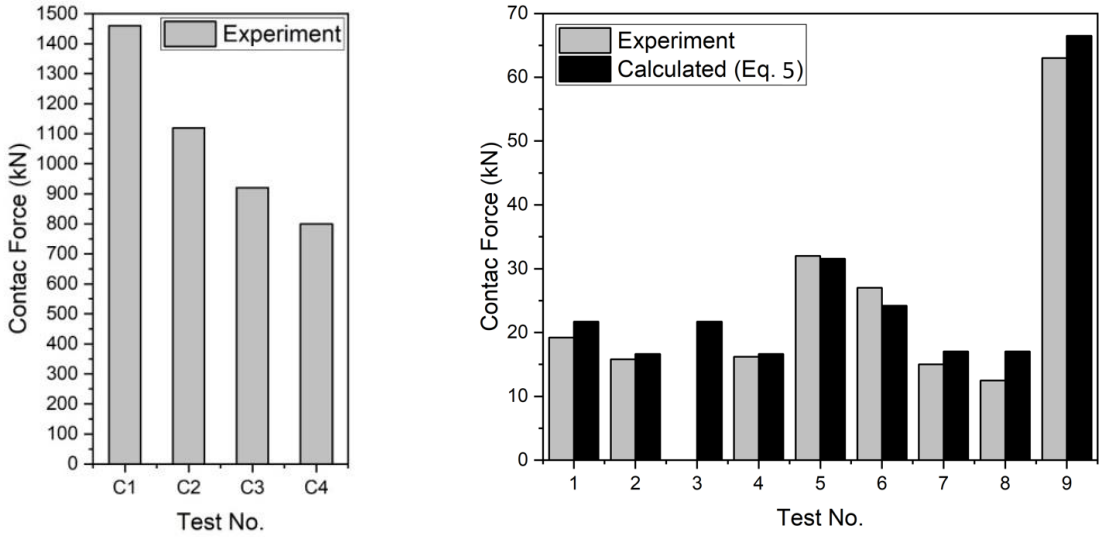


(a) Horizontal pendulum test setup (b) Vertical drop test setup

Fig. 4 vertical and horizontal impact test setups

The time-histories of the contact force delivered by the impact (i.e. the forcing function of impact) for the full-scale impact tests were obtained by multiplying the de-acceleration of the impactor by its mass. The values of the peak contact force as read off from the measured time-histories were then compared with predictions obtained from Eq. (5) demonstrating good consistencies as shown by Fig. 5 (b). These results presented further validates the accuracy of

the adopted reduction factor in full scale. Note that the data recorded from Test 3 was discarded as the measurement device was suspected to be faulty. Peak contact force values recorded from the control experiments (C1-C4) on a bare wall is also shown in Fig. 5 (a). An order of magnitude differences can be seen between test results obtained from a bare wall and a cushioned wall. The cushion layer is shown to have reduced the contact force by more than 95%.



(a) Control experiment (b) Experiments with gabion cushion protection

Fig. 5 Comparison of peak contact forces

4 Modelling of Flexural Response of The RC Wall

The term "*contact force*" refers to the peak contact force which is the maximum force experienced between the target structure / gabion cushion and the impactor at the point of contact. Most of the solutions for the peak contact force (as presented in the literature for impact action without a cushion) give a value of peak force which is transient in nature and can last for only a very short duration of time to deliver an impulse to the target. The term "*quasi-static force*" refers to the force applied to the target in order to develop the same amount of maximum deflection that can result from the impact action. This quasi-static force is equivalent to the product of the stiffness of the target and its maximum deflection resulted from the impact action.

In most impact scenarios the amplitude of the contact force can be an order of magnitude higher than the quasi-static force as illustrated in Refs. [20] and [21].

However, when the barrier is protected by a layer of cushioning material the impact action is transformed into an impulse. The amplitude and duration of the impulse depend on the design of the cushion. The transformed impulse becomes a forcing function which is then transmitted to the barrier. This forcing function has a certain natural period which may be close to the natural period of the stem wall. If these two natural periods happen to be similar significant dynamic amplification of the target structure can occur. This can result in a potential scenario where the intensity of the contact force can be equal to, or slightly lower than, that of the quasi-static force. This change is beneficial and is to do with the duration of contact being prolonged significantly. Therefore, numerical calculations based on momentum conservation similar to what is given in Ref [22] cannot be applied for determining the deflection demand of a barrier which is protected by a layer of cushioning material.

4.1 Two-degrees-of-freedom (2DOF) system

The Modified Swiss Equation (Eq. (5)) that has been introduced, and validated, provides predictions of the peak contact force which is transmitted to the surface of a RC wall which is protected by gabions. The next step is to model the time-history of the contact force which is referred herein as the forcing function. Modelling the impact generated forcing function is accomplished by the use of a spring connected lumped mass model which is made up of two lumped masses. Hence, the model is described as a two-degrees-of-freedom (2DOF) system as depicted in Fig. 6. Excel spreadsheet calculations with standard row and column operations are used in the 2DOF calculation process which can be used conveniently by practising engineers in the design office environment [23]. The amount of force that is taken up by the frontal spring of the 2DOF system represents the impact generated contact force (F_c). The two lumped masses are: (i) the lumped mass representing the impactor which is connected to the frontal spring (m)

and (ii) the lumped mass representing a portion of the gabion cushion and the effective mass of the RC cantilevered wall (m_2) which is connected to its support through the rear spring. The layer of granular material is considered to possess response behaviour likened that of viscoelastic plastic indentation behaviour as reported in Refs. [24, 25]. Thus, the frontal spring is taken to possess hysteretic properties as defined by the Hunt and Crossley model whereas the rear spring is modelled to behave in a linear elastic manner assuming that the RC stem wall responds within the limit of yield. It is important to note that the Hunt and Crosley model has only been used for modelling hard impact. This paper explores the applicability of the same contact force model for simulating soft impact and is a novel feature of this article.

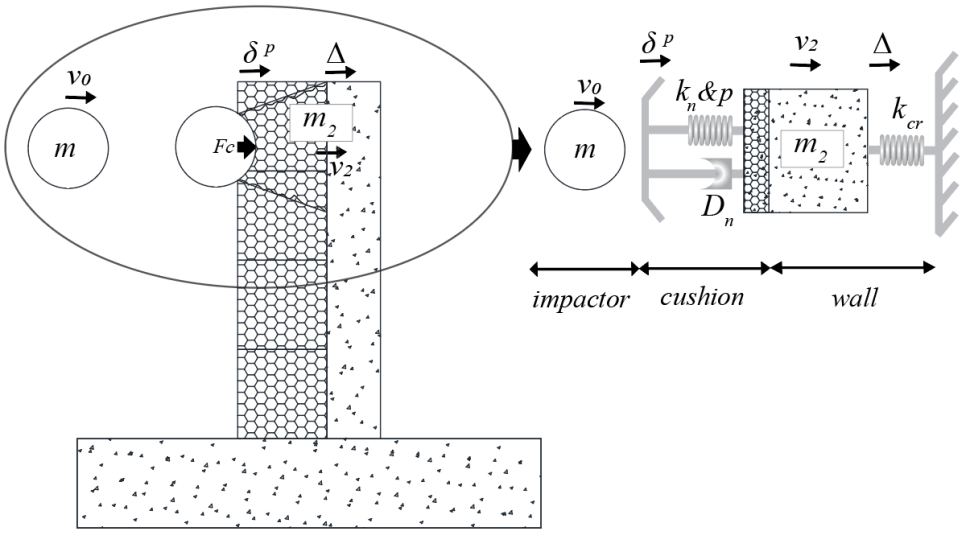


Fig. 6 2DOF simplification

4.2 Combined mass of the wall and cushion (m_2)

The second lumped mass (m_2) which is supported by the rear spring represents a portion of cushioning material in the vicinity of the point of contact in combination with the participating mass of the cantilevered wall. Selection of values for lumped mass (m_2) is usually straightforward for a solid target. However, in this case, both the gabion cushion (m_{gabion}) and the cantilevered wall (m_{wall}) may be considered to be part of the "target". Thus, the combined mass participating in the response to the impact can be represented by Eq. (6). The gabion

cushion and the RC stem wall are considered as separate structures responding to the impact action.

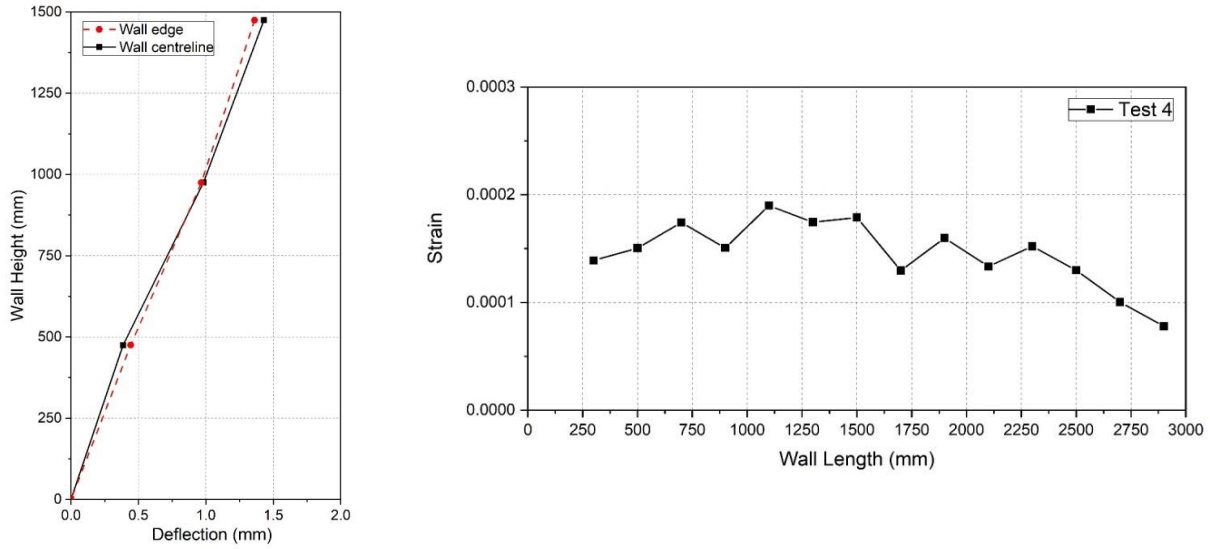
$$m_2 = m_{wall} + m_{gabion} \quad (6)$$

The portion of the cushion material that is activated by the impact in the immediate surroundings of the point of contact has been found to be funnel in shape [9, 14, 26]. For crushed rocks, the angle of the funnel may be taken as 30° as per recommendations reported in Refs.[9, 14]. According to Stoffel [15], this value can vary from 33° to 47°. However, what has been reported in the literature is only limited to horizontally layered crushed rock particles. This angle could be different for cushion materials that are confined in a gabion cage. Experiments have been conducted to determine the amount of contributory mass of the gabion cushion by the author as given in Ref [13]. It was identified that the funnel of the activated mass of particles in a layer of gabions had an angle in the range: 20° - 37°, and the angle would not vary significantly with changes in the fill material type. The smaller the angle the lesser the contributory mass of the gabion cushion in developing inertial resistance. Hence, 20° is recommended to be taken as the design funnel angle of the gabion cushion to result in a conservative prediction. The activated or participating mass of the gabion cushion (m_{gabion}) can be calculated using the generalised expression of Eq. (7) which is based on the volume of a funnel where r is the radius of an equivalent sphere of the impactor (radius of the contact) and r_1 is the radius of the force transmitted area (Fig. 6).

$$m_{gabion} = \frac{1}{3}\pi(r_1^2 + r_1 r + r^2)e\rho \quad (7)$$

The effective length of the wall undergoing flexural action could be taken as twice the height of the stem wall based on a distribution angle of 45° [22]. This assumed distribution has been confirmed by observing consistent readings from laser sensors and strain gauges that were placed at different locations along the length of the wall. Deflection (up the wall height at the edge and centreline) and the amount of tensile strain experienced by the reinforcing bars close to

the base is illustrated in Fig. 7 (a) and Fig. 7 (b) respectively (Test 4 is used as an example to justify this). Further validations of the cantilevered wall assumption are given in Ref [27] based on numerical simulations by LS-DYNA. Therefore, the value of m_{wall} may be taken as a quarter of the mass of the cantilever wall (650kg - lumped mass of the cantilever wall) based on established structural dynamics principles [28-30].



(a) Deflection of the wall (b) Tensile strain of longitudinal reinforcement

Fig. 7 Experimentally measured flexural response of the wall: Test 4

4.3 Rear spring (k_{cr})

Stiffness of the RC stem wall as derived from the principles of structural dynamics takes the same form as static stiffness (for a cantilevered wall), as shown by Eq. (8) [22].

$$k_{cr} = \frac{3EI_{cr}}{h^3} \tag{8}$$

Given the wall height (h), the only parameter to be input into Eq. (8) is the flexural rigidity of the wall section (EI_{cr}) where subscript cr denotes cracked concrete and this parameter depends on the location of reinforcing bars (see Figure 1 (b) for details). Moment-curvature analyses have been undertaken using program Response 2000 [31] for calculating the value of EI_{cr} of the tested wall section. Apart from the moment curvature analysis, a simplified method of

calculation employing Eqs. (9) to (11) can also be used for calculating the value of EI_{cr}. There are two underlying assumptions: 1) the tensile longitudinal reinforcement of the stem wall must be responding within the limit of yield and 2) there is no occurrence of any signs of brittle failure on the wall. Eq. (9) is based on the well-established Whitney stress block model (as introduced in Ref. [32]) whereas Eq. (10) was derived from Priestley, Calvi and Kowalsky [33] based on extensive moment-curvature analyses on a lightly (axially) loaded structural elements consistent with the conditions of the cantilevered wall. The estimated value of EI_{cr} is translated to $k_{cr} = 14379\, kN/m$ which represents the flexural stiffness of the RC stem wall in cracked conditions.

$$M_y = \phi M_u = 0.8 A_{st} f_y d \left(1 - 0.6 \frac{A_{st} f_y}{B d f_c'}\right) \tag{9}$$

$$\phi_y = \frac{1.7 \varepsilon_{sy}}{D} \tag{10}$$

$$EI_{cr} = \frac{M_y}{\phi_y} \tag{11}$$

4.4 Frontal spring

Parameters characterising the frontal spring (as per Hunt & Crossley Model) are namely the spring stiffness k_n, exponent p and damping coefficient D_n as shown by Eq. (12). Different expressions for determining the value of D_n can be found in the literature [34-38] Eq. (13) which was derived recently presents D_n as function of k_n and p [39-41]. $\dot{\delta}_0 = v_0$ may be assumed for input into Eq. (13) given that the barrier is initially at rest.

$$F_c = k_n \delta^p + D_n \delta^p \dot{\delta} \tag{12}$$

$$D_n = (0.2p + 1.3) \left(\frac{1 - \mathrm{COR}}{\mathrm{COR}}\right) \frac{k_n}{\dot{\delta}_0} \tag{13}$$

The expression of Eq. (14) for determining the value of the COR parameter is based on Newton's impact hypothesis. More details of this derivation are given in Ref [42].

$$\mathrm{COR} = \frac{v_1 + v_2}{v_0} \tag{14}$$

where v_1 is the velocity of the boulder on rebound (in the opposite direction of the impact), and v_2 is the velocity of the idealised lumped mass representing the responding cantilevered wall and the loaded portion of the gabion (Fig (6)).

Solution to Eq. (12) for the value of maximum contact force (F_{cmax}) is presented in the form of a closed from expression as shown by Eq. (15) which was first introduced in Ref [20]. Details of the derivation can be found in Appendix B. Parameter λ_2 which appears in Eq. (15) is introduced herein to denote the ratio of the combined target mass (i.e. m_2 as defined by Eq. (6)) and the mass of the impactor (i.e. m_2/m)).

$$F_{cmax} = k_n \left[1 + (0.2p + 1.3)\left(\frac{1-\mathrm{COR}}{\mathrm{COR}}\right)\left(\frac{-b+\sqrt{b^2+4c}}{2}\right)\right] \times \left(\frac{p+1}{2k_n}\left(\frac{\lambda_2}{1+\lambda_2}\right) m v_0^2 \mathrm{COR}\right)^{\frac{p}{p+1}} \times \left[1 - \left(\frac{-b+\sqrt{b^2+4c}}{2}\right)^2\right]^{\frac{p}{2}} \tag{15}$$

where $b = \frac{p \times \mathrm{COR}}{(1+p)(0.2p+1.3)(1-\mathrm{COR})}$ and $c = \frac{1}{p+1}$

The value of COR can be determined from experimental measurements of the velocity of motion of the impacted objects. Alternatively, a method for finding the value of COR in an elastoplastic contact has been proposed by Thornton [43]. Neither method is suited to situations where the response time of the cantilevered wall of the barrier (wall placed behind the cushion) is too short in comparison with the much prolonged compression of the cushioning material. It was observed from video capture of the cushioned impact that the impactor became attached to, or embedded into, the gabion cushion. Thus, in theory, COR = 0 may be assumed. However, the value of D_n as defined by Eq. (13) would be mathematically undefinable if COR = 0. To circumvent this issue, a very small value of COR (= 0.01) has been taken. Fig. 8 compares contact force occurring on impact as recorded by the accelerometer in Test 4 with predictions

from the 2DOF model assuming different values of COR. It was found from a sensitivity analysis that varying the value of COR in the range 0.01 - 0.2 would result in insignificant changes to the simulated behaviour of the target.

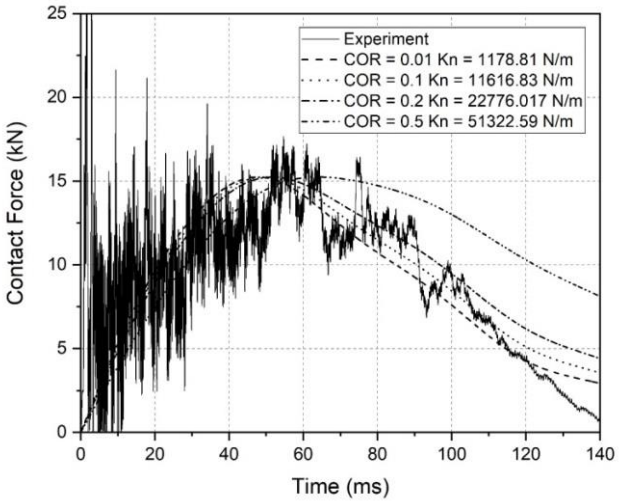


Fig. 8 Sensitivity analysis to changes in the value of COR: Test 4

The deformation behaviour of the cushion layer can be modelled assuming viscoelastic plastic behaviour when subject to an impact action [24, 25, 44]. To simplify the computations linear viscoelastic behaviour (i.e. $p = 1$) may be assumed whereas the assumption of non-linearity on contact (i.e. $p > 1$) would delay the occurrence of the rise of the contact force. No such "delay" phenomenon was observed from the impact tests. Three types of forcing functions are shown for comparison in Fig. 9 based on taking $\mathrm{COR} = 0.01$. It was found from sensitivity analyses in which the value of p was varied within the range: $1 < p < 2$ that the simulated response behaviour matched best with experimental recorded behaviour when $p = 1$ was assumed. The contact force model of Eq. (12) is accordingly simplified into Eq. (16).

$$F_c = k_l\delta + D_l\delta\dot{\delta} \tag{16}$$

where k_l is the linear spring stiffness and D_l is the damping coefficient ($k_n = k_l$ and $D_n = D_l$ when p = 1). The value of parameter D_l may be found using Eq. (17) which is a special case with p (= 1) and COR (= 0.01) based on the generalised relationship of Eq. (13).

$$D_l = 148.5\frac{k_l}{\dot{\delta}_0} \tag{17}$$

In Fig. 9, the forcing function that has been simulated as per the special case of Hunt & Crossley model based on Eq. (16) and Eq. (17) is shown by a thicker line ($p = 1$) .The comparison between the predicted and recorded forcing functions only shows order of magnitude agreement (as the high level of noise that has been recorded is not featured in the predictive model). Note that the results presented here have already been filtered using a Butterworth filter to remove high-frequency noise. The noise in experimental results is to do with the impactor touching with the rock particles and causing them to slip.

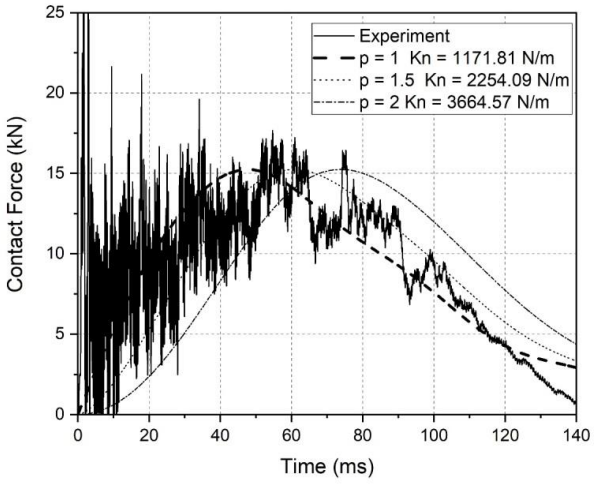


Fig. 9 Sensitivity to change in the value of p: Test 4

Take $p = 1$ and $\mathrm{COR} = 0.01$ as justified earlier. Notation is changed from k_n to k_l. Eq. (15) is then simplified into Eq. (18).

$$F_{cmax} = k_l \times \left(\frac{1}{k_l}\left(\frac{\lambda_2}{1+\lambda_2}\right) mv_0^2\right)^{\frac{1}{2}} \times 7.5 \tag{18}$$

Eq. (18) can be rearranged into Eq. (19) in which k_l is expressed as function of the peak contact force F_{cmax} along with impact parameters: m, v_o and λ_2. The factor appearing in the denominator was found to be between 50-60. A rounded-off value of 50 is taken as this would result in a slightly more conservative estimates of the stiffness, and hence contact force.

$$k_l = \frac{{F_{cmax}}^2}{50mv_0^2} \times \left(\frac{1+\lambda_2}{\lambda_2}\right) \tag{19}$$

In summary, the value of k_l can be found using Eq. (19) once the peak contact force (F_{cmax}) is known. The value of F_{cmax} can be estimated using the Modified Swiss Equation of Eq. (5) which in turn requires knowledge of the modulus of subgrade reaction (M_E). The method of obtaining M_E by static testing has been presented in section 2. The comparison between the numerically simulated and calculated values of k_l (by Eq. (19)) is presented in the form of a bar chart as shown in Fig. 10. It is shown that predictions for the value of k_l as obtained from the use of Eq. (19) are only slightly higher, and hence more conservative, than results inferred from numerical simulations of the 2DOF system model.

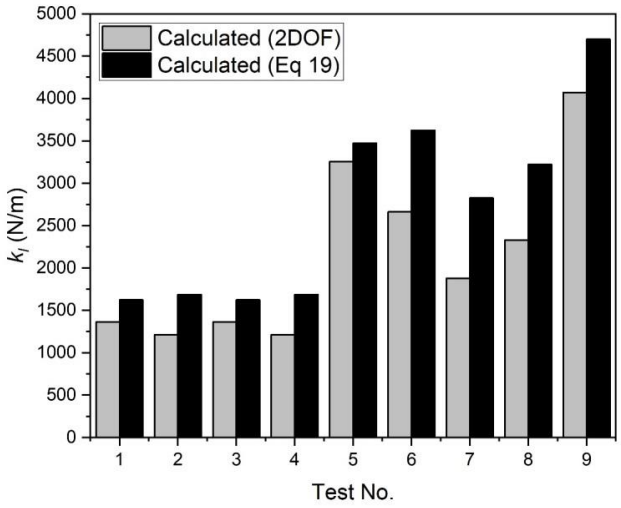


Fig. 10 Comparison of k_l calculated using 2DOF model with predictions from Eq. (19)

4.5 The deflection of the RC stem wall

Having determined the value of k_l, p and COR (hence D_l) the deflection time-histories of the responding target can be simulated (using the 2DOF system model) for comparison with time-histories recorded from the impact experiments. The proposed analytical model has been validated further by comparison of the experimentally recorded deflection of the RC wall with model predictions (as indicated by the movement of the rear lumped mass in the 2DOF model). The deflection of the RC stem wall was monitored by laser sensors which were mounted up the height of the wall at the centreline. In Fig. 11, reasonable agreement between the simulated and the recorded time-history deflection data from Test 4 is demonstrated.

In Fig. 12, maximum deflection values of the wall as inferred from the recorded time history data are shown alongside analytical predictions from the 2DOF system model for all the cushioned impact tests that have been conducted. The ability of the analytical model to give reasonably accurate predictions of the deflection demand of the RC stem wall is well demonstrated. Deflection demand of the wall without a protective cushion layer (control experiment) is also presented in Fig. 12 for comparison purposes. The presented results demonstrate that the maximum deflection of the wall with a protective cushion layer is much lower than the control experiment of the bare wall. The amount of reduction in deflection was more than 70% in most cases.

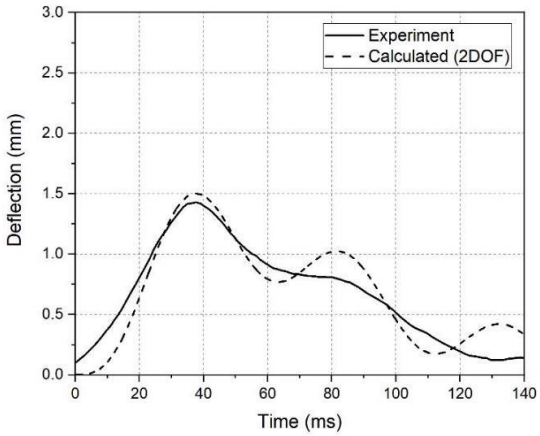


Fig. 11 Comparison of time-histories of deflection at top middle of the wall for Test 4

Yield deflection is also presented in the same figure which was calculated based on the wall properties prior to the experiment. Given that the value of the yield curvature (ϕ_y) of the cantilevered wall has been calculated using Eq. (10), being 0.021 rad/m, the value of the yield deflection (Δ_y) can be estimated using Eq. (20) and Eq. (21) as established on Ref [45], being 15.5 mm. In this, h_i represents the impact height and not to be confused with the wall height h (h_i is slightly lower than the wall height h).

$$\Delta_{yi} = \frac{\phi_y h_i^2}{3} \tag{20}$$

$$\Delta_y = \Delta_{yi}\left(\frac{3h - h_i}{2h_i}\right) \tag{21}$$

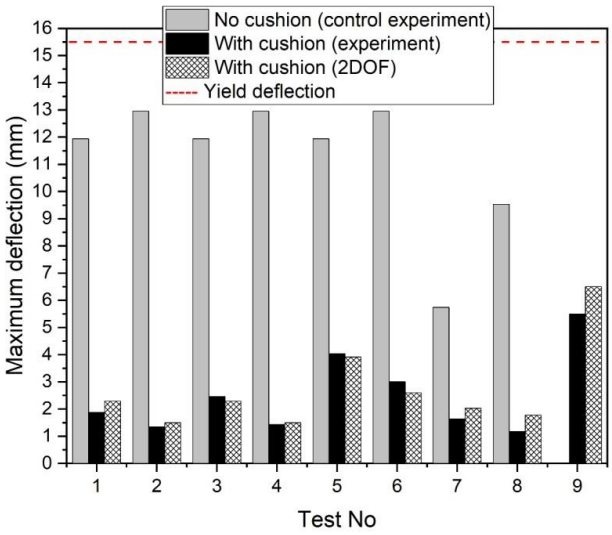


Fig. 12 Comparison of experiment and prediction of 2DOF model for maximum deflection at top middle of wall

5 A Simplified Analytical Procedure

A displacement-based model was developed by Lam, Yong, Lam, Kwan, Perera, Disfani and Gad [46] to predict the performance behaviour of reinforced concrete barrier when subjected to the impact of a boulder on the cantilevered wall causing it to deflect and bend. Detailed descriptions and derivations of the model by the authors and co-workers have been reported in the literature [47-50].

The analytical model of Eq.(22) for estimating the displacement demand of an impact has been derived, and experimentally validated, for conditions where the target is responding within the elastic limit [46]. Input to the equation is the impactor mass (m), stiffness of the target responding within the elastic limit (k), generalised mass of the target (λm), and coefficient of restitution (COR). For specific conditions where the impactor does not rebound (i.e. COR = 0) but is instead embedded into the surface of the target Eq.(22) is reduced to Eq.(23) which was first presented in Ref. [50].

If the target is a lightly loaded RC element such as a RC stem wall which is susceptible to cracking on impact "k" is replaced by "k_{cr}" where subscript "cr" denotes cracked concrete. In

the case of an impact that is cushioned by a layer of gabion Eq. (23) is modified further into Eq. (24) in which the γ factor is introduced to allow for the mitigation effects of the impact action resulted from the gabion cushion delaying the transmission of momentum to the barrier. The second term on the right-hand side of Eq.(24) which is similar in form to the right hand side of Eq.(23) can be used to estimate the deflection demand of an impact scenario where the flying object becomes attached to (or embedded into) the surface of the target (i.e. COR = 0). This assumption is supported by observations from all the tests conducted by the investigators when cushioning was put in place. Note also that the mass ratio of the target ($\lambda = \frac{m_{wall}}{m}$) is denoted herein as $\lambda_2 = \frac{m_2}{m}$ in Eq. (24) to facilitate the effect of cushioning as a combined target mass.

$$\Delta \sim \frac{mv_0}{\sqrt{mk}} \sqrt{\lambda \left(\frac{1+\mathrm{COR}}{1+\lambda}\right)^2} \qquad \text{as derived in Refs. [32] \& [56]} \qquad (22)$$

An important distinction between Eq. (22) and (23) rests with the condition of impact and rebound. Eq. (22) deals with the impactor rebounding from the target after making a one-off contact. In contrasts, Eq. (23) deals with the impactor becoming attached to the target forming a combined mass. As the latter condition is consistent with that of a cushioned impact, Eq. (23) is modified into Eq. (24) to incorporate the γ multiplier to take into account the further reduction of the displacement demand resulted from cushioning. The alternative derivation by Refs. [38] and [40] suggests that the maximum deflection is proportional to the impactor momentum at impact and that rebound is negligible.

$$\Delta \sim \frac{mv_0}{\sqrt{mk(1+\lambda)}} \qquad \text{as derived in Ref. [40]} \qquad (23)$$

$$\Delta \sim \gamma \frac{mv_0}{\sqrt{mk_{cr}(1+\lambda)}} \qquad \text{as derived in Ref. [38]} \qquad (24)$$

One of the main functionalities of the cushion is to delay the transfer of momentum thereby resulting in a further reduction in the deflection demand of the impact. The γ factor (the first

term in Eq. (24)) is to represent this further reduction which is resulted from the delay and is shown to be correlated with the time taken for the contact force to rise to its peak (i.e. "*rise time*") in the forcing function. The time taken by the target to deflect to the full extent in response to the impact is the "*response* time". The ratio of *rise time*: *response time* can be represented by the natural period ratios (T_m/T_{m_2}) of the two lumped masses in the two-degree-of-freedom (2DOF) system representation.

The value of the γ factor can be found by applying the following calculation:

1. Calculation for determining the value of T_m/T_{m_2} using Eq. (25) and
2. Calculation for determining the value of γ as function of T_m/T_{m_2} and λ_2 using the chart of Fig. 13

$$\frac{T_m}{T_{m_2}} = 2\pi\sqrt{\frac{mk_{cr}}{m_2 k_l}} \tag{25}$$

where m, m_2, k_{cr} and k_l (or k_n) are as defined in Fig. 6. The chart was developed from a parametric study which involved analyses making use of the 2DOF system as introduced in Section 4.

The value of k_l which characterises the cushion stiffness must be known beforehand in determining the value of $\frac{T_m}{T_{m_2}}$ based on use of Eq. (25). Parameter k_l can be found by use of Eq. (19).

In summary, the deflection demand of the impact can be calculated using the closed-form expression of Eq. (24) along with the design chart of Fig. 13 for identifying the value of γ. The trends of γ varying with changes in the natural period ratio (T_m/T_{m_2}) and mass ratio (λ_2) as obtained from parametric studies (based on numerical simulations of the 2DOF model) are well displayed on this chart.

The deflection demand of the cushioned impact as obtained from the calculation procedure as described have been compared with experimentally recorded results in Fig. 14. The deflection demand recorded from tests is shown to be in good agreement with analytical predictions.

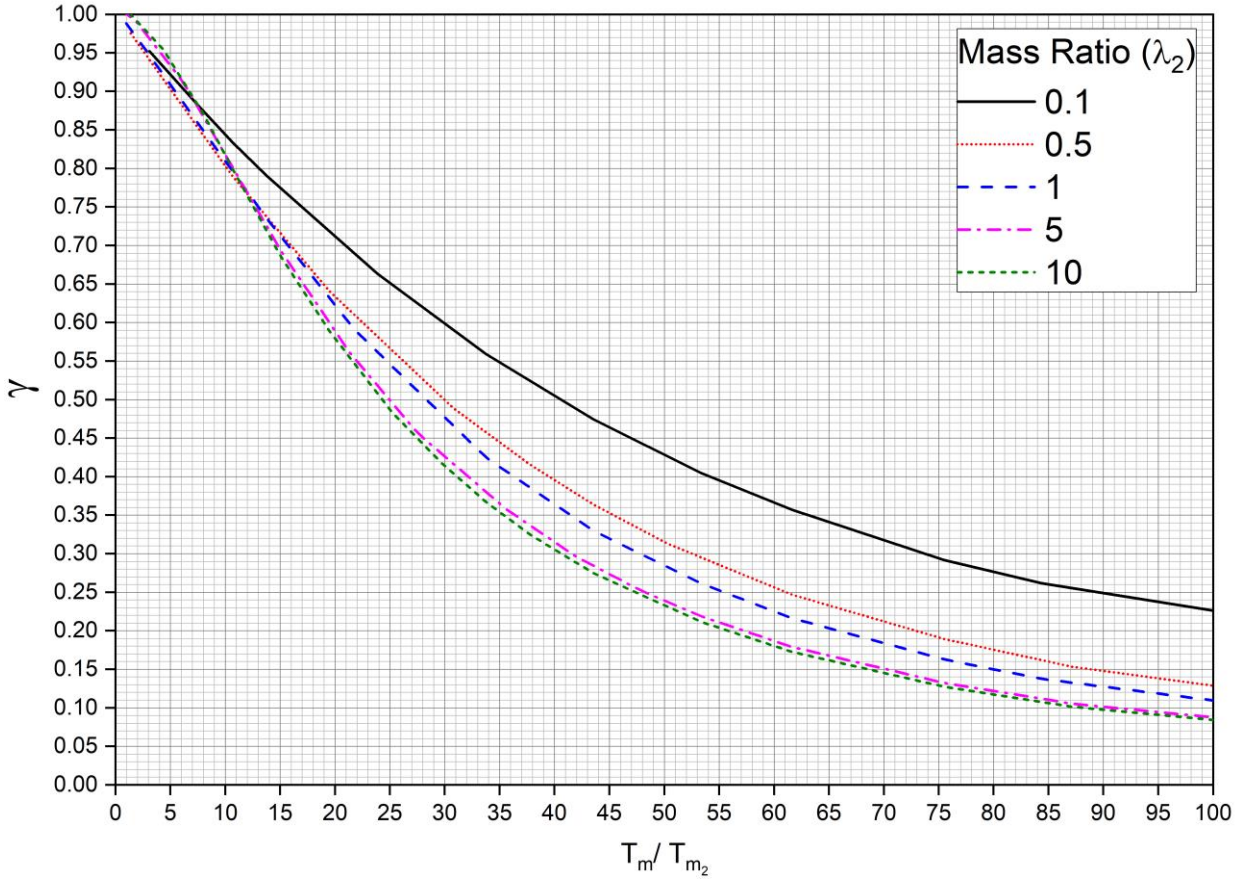


Fig. 13 Design chart for γ

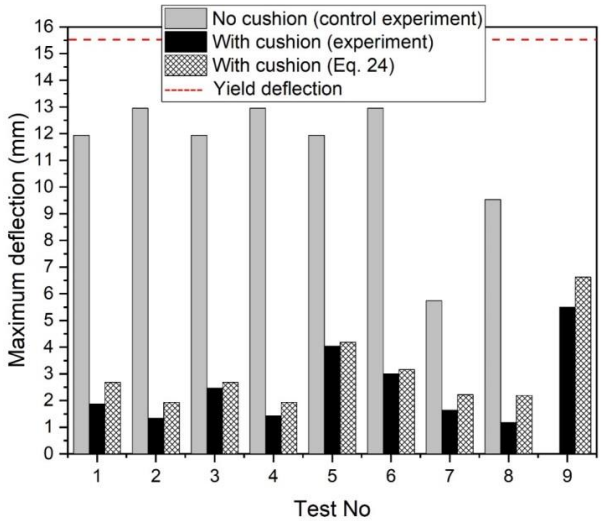


Fig. 14 Comparison of deflection recorded from experiment with predictions from Eq. (24)

6 Conclusion

Pendulum style impact tests have been performed on a full-scale reinforced concrete barrier specimen which had the protection of a layer of gabion (cushion) cover of two different filling materials. Results show that the cushion layer was able to reduce the contact force by more than 95% and deflection demand on the RC stem wall by about 70%. The particle properties of the filling material had no significant influence on the amount of reduction whereas a stronger gabion cages (built of larger diameter wire mesh) showed less reduction of the deflection demand of the impact compared to that of more flexible gabion cages. High energy impact (10kJ) test highlights the significance of the mitigation actions of the gabion cushion in terms of reduction in the contact force and the flexural action on the stem wall.

An expression for estimating the magnitude of the contact force transmitted across the thickness of the cushion was first presented and experimentally validated. It is shown that the forcing function of impact affecting the cantilevered wall (which was placed behind the cushion) could be simulated reasonably accurately by employing the non-linear viscoelastic model (also known as Hunt and Crossley model) for characterising the hysteretic properties of the frontal spring forming part of the two-degrees-of-freedom (2DOF) spring connected lumped mass system. The 2DOF system model so derived has been validated by comparison of the simulated deflection demand with experimental measurements. A closed form expression which is used in conjunction with a design chart has been derived from deflection demand data (that was generated from parametric studies employing the 2DOF system model) to facilitate uptake in design practices. A worked example is given at the Appendix A for ease reference of the proposed methodology.

This article deals with quantifying the mitigation actions of the gabion materials on the deflection demand on the stemwall of a rockfall barrier in an impact scenario. This is an original contribution as no similar initiatives has been reported in the literature. The provision of a hand calculation procedure involving the use of a design chart is an added original feature to the

presented design methodology which is limited to conditions where the stemwall responds within the limit of yield and there is no sign of occurrence of brittle fracture. Another limitation of the procedure is that the wall is not too flexible that it becomes necessary to take into account effects of the higher modes.

There are scopes for further investigations for modelling the deflection demand on the cushion protected stem wall taking into account the effects of multiple strikes at the same position on the cushion and further developing the methodology by testing wall specimens to respond beyond the yield limit.

7 References

[1] R. Chikatamarla, J. Laue, S. Springman, Rockfall impact on protection galleries, in: Second International Conference of Structural Engineering Mechanics and Computations, Balkema, Rotterdam, Cape Town, South Africa, 2004, pp. 1139-1144.

[2] A. Heymann, M. Collombet, S. Lambert, P. Gotteland, Use of external testing methods to assess damage on rockfall protection structures, in: Applied Mechanics and Materials, Trans Tech Publ, 2011, pp. 704-709.

[3] S. Lambert, A. Heymann, P. Gotteland, F. Nicot, Real-scale investigation of the kinematic response of a rockfall protection embankment, Natural Hazards and Earth System Sciences, 14 (2014) p. 1269-p. 1281.

[4] C. Ng, C.E. Choi, Y. Su, J. Kwan, C. Lam, Large-Scale Successive Boulder Impacts on a Rigid Barrier Shielded by Gabions, Canadian Geotechnical Journal, (2016).

[5] F. Calvetti, C. Di Prisco, M. Vecchiotti, Experimental and numerical study of rock-fall impacts on granular soils, Rivista Italiana di Geotecnica, 4 (2005) 95-109.

[6] N. Kishi, H. Konno, K. Ikeda, K. Matsuoka, Prototype impact tests on ultimate impact resistance of PC rock-sheds, International Journal of Impact Engineering, 27 (2002) 969-985.

[7] V. Labiouse, F. Descoeudres, S. Montani, C. Schmidhalter, Experimental study of rock blocks falling down on a reinforced concrete slab covered by absorbing cushions, Revue française de géotechnique, 69 (1994) 41-61.

[8] K. Schellenberg, A. Volkwein, A. Roth, T. Vogel, Rockfall–Falling weight tests on galleries with special cushion layers, in: Proceedings, 3rd international conference on protection of structures against hazards, September, 2006, pp. 28-29.

[9] F. Calvetti, Distinct Element evaluation of the rock-fall design load for shelters, Rivista Italiana di geotecnica, 3 (1998) 63-83.

[10] H. Yoshida, Recent experimental studies on rockfall control in Japan, in: Joint Japan-Swiss Scientific Seminar on Impact Load by Rock Falls and Design of Protection Structures, Kanazawa, Japan, 1999.

[11] R. Agostini, Flexible gabion structures in earth retaining works, Officine Maccaferri, 1987.

[12] H. Hertz, Über die Berührung fester elastischer Körper. On the contact of elastic solids, Reine und angewandte Mathematik. London:(Instruction anglaise dans Miscellaneous papers by H. Hertz) Eds Jones et Schaott, in, Macmillan, 1896.

[13] J.S. Perera, N. Lam, M.M. Disfani, E. Gad, Impact response behaviour of gabion cells filled with different cushion, in: ACMSM25, Brisbane, 2018.
[14] ASTRA, Einwirkungen infolge Steinschlags auf Schutzgalerien, Richtlinie, Bundesamt für Strassen, Baudirektion SBB, Eidgenössische Drucksachen- und Materialzentrale, Bern., (2008).
[15] S.M. Stoffel, Sollicitation dynamique de la couverture des galeries de protection lors de chutes de blocs, in, Verlag nicht ermittelbar, 1998.
[16] K. Bucher, Dynamische Berechnung von Steinschlageinwirkungen, in: Proceedings, Schweizerische Gesellschaft für Boden und Felsmechanik, Conference Paper Montreux, 1997.
[17] S. Degago, R. Ebeltoft, S. Nordal, Effect of rock fall geometries impacting soil cushion: a numerical procedure, in: proceedings of the 12th International Conference of International Association for Computer Methods and Advances in Geomechanics (IACMAG), Goa, India, 2008, pp. 1-6.
[18] V. Labiouse, F. Descoeudres, S. Montani, Experimental study of rock sheds impacted by rock blocks, Structural Engineering International, 6 (1996) 171-176.
[19] D.-G. Lin, Y. Lin, F. Yu, Deformation analyses of gabion structures, INTERPRAEVENT 2010, (2010) 512-526.
[20] J. Sun, Lam, N., Zhang, L., Ruan, D. and Gad, E., Contact forces generated by hailstone impact, International Journal of Impact Engineering, 84 (2015) 145-158.
[21] S. Perera, Lam, N., Pathirana, M., Zhang, L., Ruan, D. and Gad, E., Deterministic solutions for contact force generated by impact of windborne debris, International Journal of Impact Engineering, 91 (2016) 126-141.
[22] A.C. Yong, N.T. Lam, S.J. Menegon, E.F. Gad, Experimental and Analytical Assessment of Flexural Behavior of Cantilevered RC Walls Subjected to Impact Actions, Journal of Structural Engineering, 146 (2020) 04020034.
[23] N. Lam, H. Tsang, E. Gad, Simulations of response to low velocity impact by spreadsheet, International Journal of Structural Stability and Dynamics, 10 (2010) 483-499.
[24] C. Di Prisco, M. Vecchiotti, A rheological model for the description of boulder impacts on granular strata, GEOTECHNIQUE-LONDON-, 56 (2006) 469.
[25] R. Chikatamarla, Optimisation of cushion materials for rockfall protection galleries, PhD Dissertation, vdf Hochschulverlag AG, 2007.
[26] Japan Road Association, Manual for anti-impact structures against falling rocks (in Japanese). (1983).
[27] A.C.Y. Yong, Impact-resistance of Reinforced Concrete Structures, in, 2019.
[28] J.S.P. Pethati Mudiyanselage Don, Rigid Barrier with a Gabion Cushion Subjected to Boulder Impact, in, 2019.
[29] J. Sun, N. Lam, L. Zhang, D. Ruan, E. Gad, Computer Simulation of Contact Forces Generated by Impact, in: International Journal of Structural Stability and Dynamics, 2016.
[30] A.C.Y. Yong, Closed-form Expressions for Improved Impact Resistant Design of Reinforced Concrete Beams, Structures, (2021).
[31] E.C. Bentz, Sectional analysis of reinforced concrete members, University of Toronto Toronto, 2000.
[32] R. Park, T. Paulay, Reinforced concrete structures, John Wiley & Sons, 1975.
[33] M.J.N. Priestley, G.M. Calvi, M.J. Kowalsky, Displacement-Based Seismic Design of Structures, IUSS Press, Pavia, Italy, 2007.
[34] R.G. Herbert, D.C. McWhannell, Shape and Frequency Composition of Pulses From an Impact Pair, Journal of Manufacturing Science and Engineering, 99 (1977) 513-518.
[35] T.W. Lee, A.C. Wang, On The Dynamics of Intermittent-Motion Mechanisms. Part 1: Dynamic Model and Response, J. Mech. Des., 105 (1983) 534-540.
[36] H.M. Lankarani, P.E. Nikravesh, A contact force model with hysteresis damping for impact analysis of multibody systems, J. Mech. Des., 112 (1990) 369-376.

[37] Y. Gonthier, J. McPhee, C. Lange, J.C. Piedboeuf, A regularized contact model with asymmetric damping and dwell-time dependent friction, Multibody Syst. Dyn., 11 (2004) 209-233.
[38] P. Flores, M. Machado, M.T. Silva, J.M. Martins, On the continuous contact force models for soft materials in multibody dynamics, Multibody Syst. Dyn., 25 (2011) 357-375.
[39] J. Sun, N. Lam, L. Zhang, D. Ruan, E. Gad, Contact forces generated by hailstone impact, International Journal of Impact Engineering, 84 (2015) 145-158.
[40] S. Perera, N. Lam, M. Pathirana, L. Zhang, D. Ruan, E. Gad, Deterministic solutions for contact force generated by impact of windborne debris, Int. J. Impact Eng., 91 (2016) 126-141.
[41] S. Perera, N. Lam, M. Pathirana, L. Zhang, D. Ruan, E. Gad, Use of static tests for predicting damage to cladding panels caused by storm debris, Journal of Building Engineering, 12 (2017) 109-117.
[42] A.C. Yong, C. Lam, N.T. Lam, J.S. Perera, J.S. Kwan, Analytical solution for estimating sliding displacement of rigid barriers subjected to boulder impact, Journal of Engineering Mechanics, 145 (2019) 04019006.
[43] C. Thornton, Coefficient of restitution for collinear collisions of elastic-perfectly plastic spheres, Journal of Applied Mechanics, 64 (1997) 383-386.
[44] C. di Prisco, M. Vecchiotti, Design charts for evaluating impact forces on dissipative granular soil cushions, Journal of geotechnical and geoenvironmental engineering, 136 (2010) 1529-1541.
[45] A.C. Yong, N.T. Lam, S.J. Menegon, E.F. Gad, Cantilevered RC Wall Subjected to Combined Static and Impact Actions, International Journal of Impact Engineering, (2020) 103596.
[46] N.T. Lam, A.C. Yong, C. Lam, J.S. Kwan, J.S. Perera, M.M. Disfani, E. Gad, Displacement-based approach for the assessment of overturning stability of rectangular rigid barriers subjected to point impact, Journal of Engineering Mechanics, 144 (2017) 04017161.
[47] N.T.K. Lam, A.C.Y. Yong, C. Lam, J.S.H. Kwan, J.S. Perera, M.M. Disfani, E. Gad, Displacement-based approach for the assessment of overturning stability of rectangular rigid barriers subjected to point impact, Journal of Engineering Mechanics, 144 (2018).
[48] N. Lam, E. Gad, The estimation of impact forces based on first principles, in: Australasian Structural Engineering Conference: ASEC 2016, Engineers Australia, 2016, pp. 350.
[49] Y. Yang, N.T.K. Lam, L. Zhang, Evaluation of simplified methods of estimating beam responses to impact, International Journal of Structural Stability and Dynamics, 12 (2012) 1250016-1250011-1250016-1250024.
[50] M. Ali, J. Sun, N. Lam, L. Zhang, E. Gad, Simple hand calculation method for estimating deflection generated by the low velocity impact of a solid object, Australian Journal of Structural Engineering, 15 (2014) 243-259.
[51] S. Perera, Modelling impact actions of flying and falling objects, in, 2017.

Appendix A - worked Example for Illustration of the Simplified Procedure

The rigid barrier considered in this worked example is to withstand a rockfall event of 1.5 m diameter boulder impacting at 7 ms^{-1} velocity. The 10 m long rigid barrier is protected by 0.5 m thick gabions cushion layer which has a bulk density of 1500 kg/m^3 (Fig. A1). It is designed with 40 mm reinforcement at 200 mm spacing. Other parameters used for the design are as follows: f_c'= 32 MPa, f_y= 500 MPa, E= 200 GPa, M_E = 3000 kPa (assuming the use of strong cages as cushion) , ϕ_k= 40°. Calculation is considered on per metre length of wall basis.

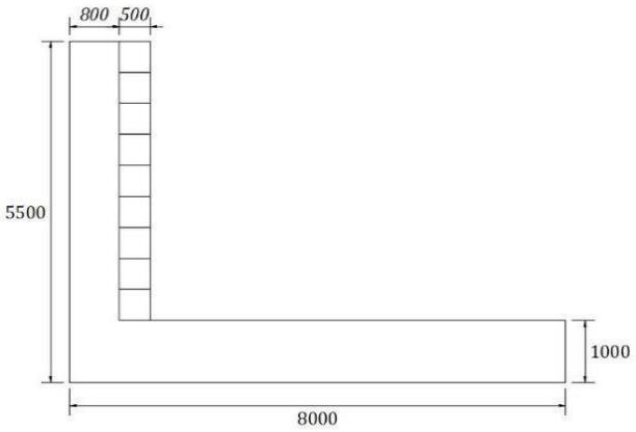


Fig. A1 Dimensions of rigid barrier

$$A_{st} = \frac{1000}{200} \times \pi \left(\frac{40}{2}\right)^2 = 6283.2\ mm^2/m$$

$$M_y = 0.8 A_{st} f_y d \left(1 - 0.6 \frac{A_{st} f_y}{B d f_c'}\right)$$

$$= 0.8 \times 6283.2 \times 500 \times 700 \times \left(1 - 0.6 \times \frac{6283.2 \times 500}{1000 \times 700 \times 32}\right) \times 10^{-6} = 1611\ kNm/m$$

$$L_{eff} = 2(h) = 2 \times (5.5 - 1) = 9\ m$$

$$M_y = 1611 \times 9\ = 14501\ kNm$$

$$\varepsilon_{sy} = \frac{f_y}{E} = \frac{500}{200000} = 0.0025;\ \phi_y = \frac{1.7\varepsilon_{sy}}{D} = \frac{1.7(0.0025)}{0.8} = 0.0053125\ rad/m$$

$$EI_{cr} = \frac{M_y}{\phi_y} = \frac{14501}{0.0053125} = 2729643\ kNm^2$$

$$k_{cr} = \frac{3EI_{cr}}{h^3} = \frac{3(2729643\ )}{4.5^3} = 89865\ kN/m$$

710 $r_1 = r + e \times tan(20°) = 0.75 + 0.5 \times tan(20°) = 0.932\ m$

711 $m_{gabion} = \frac{1}{3}\pi(r_1^2 + r_1 r + r^2)e\rho_g = \frac{1}{3}\pi(0.932^2 + 0.932 \times 0.75 + 0.75^2)0.5 \times 1500$

712 $= 1672\ kg$

713 $m_{wall} = 0.25 \times 0.8 \times 9 \times 4.5 \times 2450 = 19845\ kg$

714 $m_2 = m_{wall} + m_{gabion} = 19845 + 1672 = 21517\ kg$

715 $m\ =\ 2650 \times \frac{4}{3}\pi \times \left(\frac{1.5}{2}\right)^3\ =\ 4683\ kg$

716 $\lambda_2 = \frac{m_2}{m} = \frac{21517}{4683} = 4.59$

717 $F_{cmax} = 0.65 \times 2.8 \times e^{-0.5} \times r^{0.7} \times M_E^{0.4} \times tan\phi_k \times \left(\frac{mv_0^2}{2}\right)^{0.6}$

718 $= 1.82 \times 0.5^{-0.5} \times 0.75^{0.7} \times 3000^{0.4} \times tan40° \times \left(\frac{4.683 \times 7^2}{2}\right)^{0.6} = 747.49\ kN$

719 $k_l = \frac{{F_{cmax}}^2}{50mv_0^2} \times \left(\frac{1+\lambda_2}{\lambda_2}\right) = \frac{747.49^2}{50 \times 4683 \times 7^2} \times \left(\frac{1+4.59}{4.59}\right) = 59298\ N/m$

720 $T_m = 2\pi\sqrt{\frac{m}{k_l}}\ = 2\pi\sqrt{\frac{4683}{59298}} = 1.77\ s$

721 $T_{m_2} = 2\pi\sqrt{\frac{m_2}{k_{cr}}}\ = 2\pi\sqrt{\frac{21517}{89865000}} = 0.097\ s$

722 $\frac{T_m}{T_{m_2}} = \frac{1.77}{0.097} = 18.16$; by using the design chart given in Fig. 13; $\gamma = 0.63$

723 $\Delta = \gamma \times \frac{mv_0}{\sqrt{mk_{cr}(1+\lambda_2)}} =\ 0.63 \times \frac{4683 \times 7}{\sqrt{4683 \times 89865000 \times (1+4.59)}} = 13.46\ mm$

724 $\Delta_y = \frac{\phi_y h^2}{3} = \frac{0.0053125 \times 4.5^2}{3} = 36\ mm$

725 It is concluded that:

726 $\Delta_y > \Delta$ meaning that the RC stem wall is predicted to respond within the limit of yield.

Appendix B - derivation of the Eq. 15

The non-linear force-displacement (F_c vs δ) relationship introdcued by Eq. (15) is illustrated in Fig. 1 below.

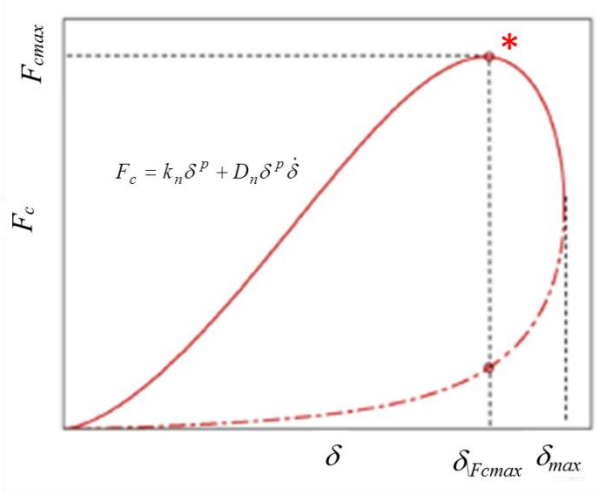


Fig. B1 Peak contact force and maximum indentation in Hunt & Crossley Model

When $\frac{\partial F}{\partial \delta} = 0$, the contact force F_c value reach to the peak value F_{cmax} as shown by Eq. (B1).

$$\frac{\partial F}{\partial \delta} = pk_n\delta^{p-1} + k_n(0.2p + 1.3)\frac{1 - COR}{COR}\frac{1}{\dot{\delta}_o}\left(p\delta^{p-1}\dot{\delta} + \delta^p\frac{\partial \dot{\delta}}{\partial \delta}\right) = 0 \qquad \text{(B1)}$$

By taking $x = \frac{\delta}{\delta_{max}}$ and $y = \frac{\dot{\delta}}{\dot{\delta}_0}$ where δ_{max} is the maximum indentation, Eq. (B1) can be simplified to Eq. B2 as shown below.

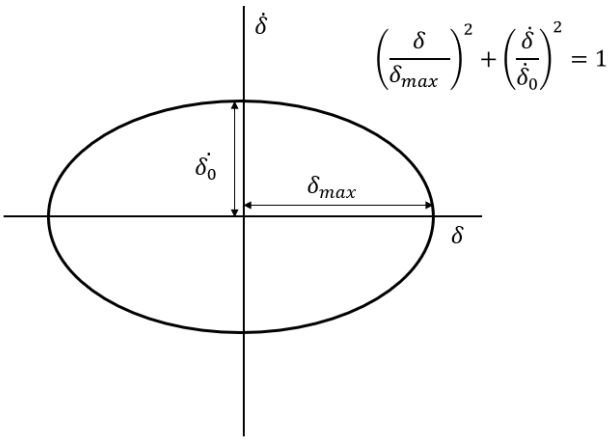
$$p + (0.2p + 1.3)\frac{1 - COR}{COR}\left(py + x\frac{\partial y}{\partial x}\right) = 0 \qquad \text{(B2)}$$

The elliptical relationship between indentation (δ) and its rate ($\dot{\delta}$) as illustrated in Fig. 2 is adopted. Since $x^2 + y^2 = 1$, $\frac{\partial y}{\partial x}$ can be solved as shown in Eq. (B3)

$$\frac{\partial y}{\partial x} = \frac{1}{2}(-2x)(1 - x^2)^{-\frac{1}{2}} = -\frac{x}{\sqrt{1 - x^2}} = -\frac{\sqrt{1 - y^2}}{y} \qquad \text{(B3)}$$

Substituting Eq. (B3) into (B2) and making use of the stated x-y relationship gives Eq. (B4).

$$py + (0.2p + 1.3)\frac{1 - COR}{COR}(py^2 - 1 + y^2) = 0 \qquad \text{(B4)}$$



738

739 **Fig. B2 Adopted relationship of indentation with rate of indentation**

740 It can be shown by some algebraic manipulations that:

$$y^2 + \left(\frac{p}{(p+1)(0.2p+1.3)} \times \frac{COR}{1-COR}\right) y - \left(\frac{1}{p+1}\right) = 0$$

741 The root of the equation (y') can be expressed as shown in Eq. (B5):

$$y' = \frac{-b+\sqrt{b^2+4c}}{2} \qquad \text{where } b = \frac{p \times COR}{(p+1)(0.2p+1.3)(1-COR)} \text{ and } c = \frac{1}{p+1} \tag{B5}$$

742 The value of the peak contact force F_{cmax} may therefore be calculated using Eq. (B6).

$$F_{cmax} = k_n \left[1 + (0.2p + 1.3)\left(\frac{1-\mathrm{COR}}{\mathrm{COR}}\right) y'\right] \times \delta_{max}^{p} \times [1 - \mathrm{y'}^2]^{\frac{p}{2}} \tag{B6}$$

743 where δ_{max}^{p} can be found using Eq. (B7) as shwon in below. The derivation of Eq. (B7) is
744 availabe in Ref [51]. This is an improved version of Eq. (2) including COR and combained
745 target mass ratio.

$$\delta_{max}^{p} = \left(\frac{p+1}{2k_n}\left(\frac{\lambda_2}{1+\lambda_2}\right) m v_0^2 \mathrm{COR}\right)^{\frac{p}{p+1}} \tag{B7}$$

746 In summary, the value of F_{cmax} (Eq. (15)) may be calculated by combining the use of Eq. (B5),
747 Eq. (B6) and Eq. (B7).